Supplementary Materials

Retention of Engineered Nanoparticles in Drinking Water Treatment Processes – Laboratory and Pilot Scale Experiments

Norbert Konradt [1,*], Laura Schneider [2], Stefan Bianga [3], Detlef Schroden [1], Peter Janknecht [4] and Georg Krekel [5,*]

[1] Stadtwerke Düsseldorf AG, Wiedfeld 50, 40589 Düsseldorf, Germany (NK, DS)
[2] NextPharma Oy, Niittyhaankatu 20, 33720 Tampere, Finland; laura.schneider@nextpharma.com (L.S.)
[3] BASF Personal Care and Nutrition GmbH, Henkelstraße 67, 40589 Düsseldorf, stefan.bianga@basf.com (SB)
[4] Enercity AG, Ihmeplatz 2, 30449 Hannover, Germany; peter.janknecht@enercity.de (PJ)
[5] Hochschule Niederrhein, Adlerstr. 32, 47798 Krefeld, Germany
* Correspondence: norbkonradt@gmx.de (NK), georg.krekel@hs-niederrhein.de (GK)

S1. Materials

Substance [1]	Supplier
Acetone	Merck
Aquazit® anthracite, type N, 1.4 – 2.5 mm, technical grade	Euroquarz, Dorsten, Germany
Aquagran ® sand 0.7 – 1.25 mm, 0.8 mm (54%), technical grade	Euroquarz, Dorsten, Germany
Bakerbond spe™ silica gel columns, 3 ml, 0.5 g	J.T. Baker®
Silica gel, pore size 60 Å, 200 – 400 mesh particle size	Merck
Calcium chloride dihydrate	Merck
Chromium(III) chloride hexahydrate, pure	Merck
Ethylene glycol (EG), spectrophotometric grade, ≥99%	Sigma-Aldrich
Glycerol, 87%	Merck
Gold (III) chloride solution, 99.99% trace metals basis, 30 wt.% in dilute HCl ($HAuCl_4$ * 4 H_2O)	Sigma-Aldrich
Gilufloc® 40, aluminum chloride/sulfate, technical grade	Aquakorin, Odenthal, Germany
Norit® ROW 0.8 Supra, activated carbon, technical grade, ground to 1 µm (46.3%)	Norit Nederland B.V., Amersfoort, The Netherlands
Hexadecyltrimethylammonium bromide (CTAB)	Sigma Aldrich
Hydrogen peroxide 30% Emprove (for pilot scale)	Merck
Iron(II) chloride tetrahydrate	Merck
Magnesium chloride hexahydrate	Merck
Mercaptopropionic acid (MPA)	Sigma Aldrich
Oxygen 3.5 (99.95%)	Air Products, Hattingen, Germany
Polyvinylpyrrolidone, average Mw 40 kDa	Sigma-Aldrich
Polyvinylpyrrolidone, average Mw 55 kDa	Sigma-Aldrich
Potassium hexacyanoferrate(III)	Merck
Silver sulphate	Merck
Silver nitrate 99.9999% trace metals basis	Sigma-Aldrich
Sodium borohydride ($NaBH_4$)	Merck

Sodium hydroxide solution 32%,	AnalytiChem GmbH, Duisburg, Germany
Sodium mercaptoethane sulfonate (MES)	Sigma Aldrich
Sodium thiosulphate	Merck
Trifloc® S, iron(III) chloride. technical grade	Aquakorin, Odenthal, Germany
Trisodium citrate dihydrate	Honeywell
Triphenylphosphine monosulfonate (TPPMS)	Sigma Aldrich
Deionized water (DI), 18.2 MΩ cm^{-1} made with Purelab Classic	ELGA LabWater Veolia Water Technologies Deutschland GmbH, Celle, Germany

[1] All reagents used were analytical grade unless otherwise stated.

S2. Synthesis and characterization of engineered nanoparticles

Gold nanoparticles can be stabilized by ligands that form the shell of the core-shell structures. The synthesis of the different NPs is various below.

S2.1. Synthesis of citrate-coated gold nanoparticles (McFarland, A. D., 2004) [1].

A stock solution of 1 mM auric acid was prepared by diluting 61.8 µL of the gold(III) chloride reagent solution in 100 mL DI. 20 mL of the prepared diluted auric acid solution was heated in a 50 mL Erlenmeyer flask with vigorous stirring and then 2 mL trisodium citrate dihydrate solution (38 mM) was added. Over the next 2 minutes, the solution turned from yellow to colorless, then to bluish purple, to purple, and finally to ruby red, indicating the formation of gold nanoparticles. A volume loss was compensated by adding deionized water to a total volume of 22 mL. The gold nanoparticle (AuNP) dispersion was cooled and stored at 15 °C. The total amount of gold was calculated to be 0.179 g L^{-1}.

S2.2. Synthesis of MPA-coated gold nanoparticles (Yonezawa et al., 1999) [2]

Citrate can be easily replaced by other ligands such as mercapto anions for higher NP stability. 10 mL MPA was diluted in 10 mL DI and titrated with NaOH (32%) to a final pH of 7.0. The final total volume was 37 mL and the MPA concentration was 5.74 M. Citrate-coated AuNPs were synthesized by preparing a 5.8 m M $HAuCl_4 * 4 H_2O$ solution (10 mL) in DI and heating to reflux. Then, 10 mL of 2 wt.% trisodium citrate and 10 mL of neutralized MPA solution were added and heated to boiling point where the solution turned ruby red. The citrate was converted to carbon dioxide while the MPA ions were bound to the gold nanoparticles. The gold concentration was calculated to be 0.571 g L^{-1}.

S2.3. Synthesis of MES-coated gold nanoparticles (Brubaker, 2006) [3]

MES-coated AuNPs were prepared by replacing the citrate shell with MES anions. 0.85 mL of 29 mM $HAuCl_4 * 4 H_2O$ was diluted with 95 mL DI and heated to boiling point. The addition of 5 mL of 1 wt.% trisodium citrate dihydrate resulted in the formation of ruby red citrate-coated AuNPs. The colloidal solution was allowed to cool before adding an excess of 2 mM MES in a molar ratio of 1:5 (20.2 mg MES dissolved in 61.63 mL DI). The dispersion was stirred for 24 hours at room temperature. The gold concentration was calculated to be 3.367 g L^{-1}.

S2.4. Synthesis of TPPMS-coated gold nanoparticles (Simon et al., 2007) [4]

Citrate-coated Au/NPs were synthesized as described in S2.1. A ligand exchange was performed using TPPMS to replace the citrate layer. Therefore, 1 mg TPPMS was added per 10 mL of 0.4 mM citrate functionalized AuNP dispersion and stirred for 5 min. The mixture was left overnight at 4 °C. The gold concentration was calculated to be 0.179 g L^{-1}.

S2.5. Synthesis of CTAB-coated gold nanoparticles Tiwari et al., 2010) [5]

AuNPs coated with a bilayer of CTAB were synthesized as follows: 10 mL of a 0.2 M dispersion of CTAB in DI with 0.5 mM $HAuCl_4$ was prepared and 0.6 mL of a 10 mM solution of ice-cold $NaBH_4$ in DI was added. The mixture was stirred for 3 hours at room temperature and then stored without stirring for 3 days. Excess CTAB was removed by filtration (Schleicher & Schüll, paper filter disks, ashless, 589/4 yellow band) before using the CTAB functionalized AuNPs. The gold concentration was calculated to be 29.9 mg L^{-1}.

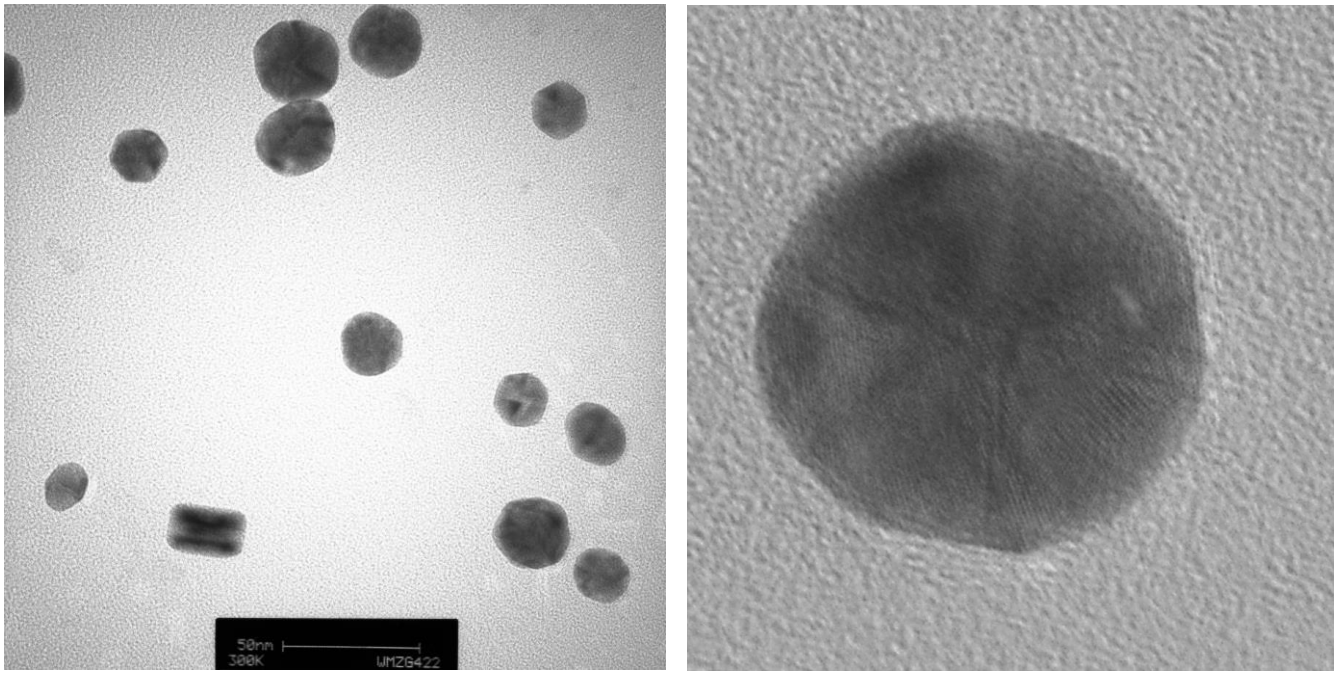
S2.6. Synthesis of PVP-coated gold nanoparticles (Joshi, 2010) [6]

PVP-coated gold nanoparticles were synthesized by dissolving 0.5 g polyvinylpyrrolidone (PVP, Mw 55 kDa) in 30 mL DI. The solution was heated to boiling and 2.5 mL of 8.8 mM trisodium citrate solution in DI was added. The mixture was boiled for another 10 minutes and then 1 mL 0.01 M $HAuCl_4$ was injected. The yellow solution immediately turns colorless and then ruby red, indicating the formation of PVP capped gold nanoparticles. The concentration of gold was calculated to be 58.8 mg L^{-1}.

Several batches of PVP-coated AuNPs were synthesized for dosage in the pilot plant using the following amounts: 1.75 g PVP, 3.14 mM sodium citrate, 0.367 mM auric acid in 175 ml DI.

The gold concentration was calculated to be 0.413 g L^{-1}.

Transmission electron microscopy (TEM) revealed that the PVP/AuNPs had a diameter of 10 to 25 nm for the gold core and their shape was mainly icosahedral (Figure S2.6.1).



(a) **(b)**

Figure S2.6.1. TEM of PVP/AuNPs; (a) distribution; (b) single icosahedral AuNPs.

The dynamic light scattering (DLS) results showed a monodisperse distribution in solution (Figure S2.6.2) with a Z-average of 59 nm for the hydrodynamic size.

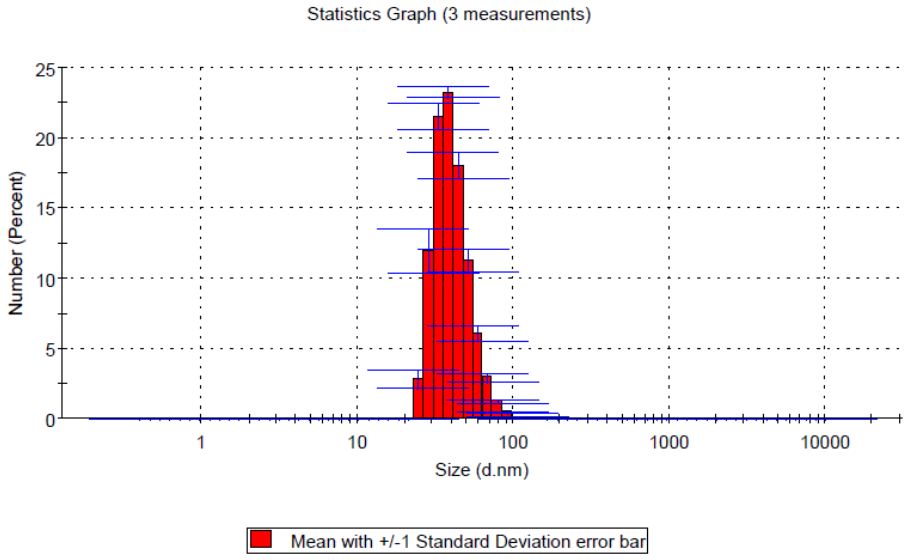


Figure S2.6.2. Size distribution of PVP/AuNPs with DLS in water at 25.0 °C.

Several batches were synthesized for dosing in the pilot plant. A typical procedure was: PVP (0.75 g) was dissolved in 125 mL DI and heated to 100 °C. 0.41 mol of trisodium citrate was added. The mixture was boiled for 10 minutes and 0.36 mmol HAuCl4 dissolved in 10 ml DI was added with stirring. The reaction mixture became clear and deep red.

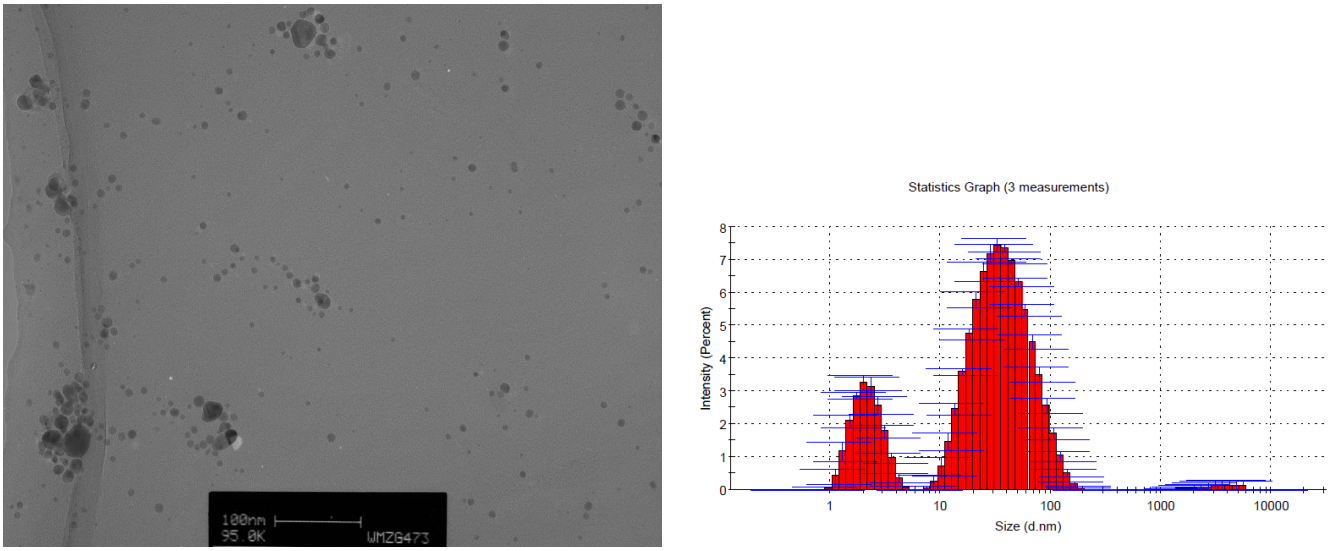
Quality control was carried out by recording a UV-Vis spectrum. The batches corresponding to the PVP/AuNP literature spectrum were combined and contained 3.09 mM Au and 13.7 g PVP in 1.85 L DI. It was diluted to 5 L DI for dispensing. For dosing in the pilot plant, the stability of the PVP/AuNPs was tested over 5 days in DI, DW and RH and found to be stable (Table S2.6).

Table S2.6. PVP/AuNP stability over 5 days.

Absorbance	DI	DW	RH
Starting value	0.347	0.282	0.322
After 5 days	0.329	0.282	0.319
Change (%)	-5.2	0.2	-1.0

S2.7.1 Synthesis of PVP-coated silver nanoparticles in glycerol/water (Elechiguerra et al., 2005) [7]

Silver nanoparticles were prepared by the polyol method using glycerol as solvent and reducing agent. PVP was used as a stabilizing agent. For the synthesis of PVP-coated AgNPs, 0.2 g of PVP (Mw 40 kDa) was dissolved in 30 mL of glycerol. The solution was heated to 140 °C under reflux and held at this temperature for 30 min before 2 mL of aqueous 15 mM silver sulfate solution was added. The solution immediately turned deep yellow, indicating the formation of PVP/AgNPs. The dispersion was stirred at 140 °C for 1 hour and then cooled to room temperature. The silver concentration was calculated to be 0.202 g L^{-1}.



(a) **(b)**

Figure S2.7.1. (a) TEM of PVP-40kDa/AgNPs; **(b)** Size distribution PVP/AgNPs with DLS at 25.0 °C in (a) Glycerol/water.

TEM showed that the PVP/AgNPs were polydisperse with a diameter of 1 to 25 nm for the silver core (Figure S2.7.1a). DLS revealed that PVP/AgNPs in glycerol/water were present in water as two fractions, one with a Z-average of 2 nm and a second with a maximum at 40 nm (Figure S2.7.1b).

S2.7.2. Synthesis of PVP-coated silver nanoparticles in EG/water (Carotenuto et al., 2000) [8]

For dosing in the pilot plant, a synthesis in EG was chosen for better upscaling. A typical procedure was as follows: 0.9 g PVP (Mw 40 kDa) was dissolved in 100 mL EG and heated to 150 °C. 1.45 mmol of $AgNO_3$ was dissolved in 10 ml

of DI and added with stirring. The reaction mixture became clear and yellow-brown. Quality control was performed by recording a UV-Vis spectrum. The UV-Vis spectrum is shown in Figure S2.7.2.1.

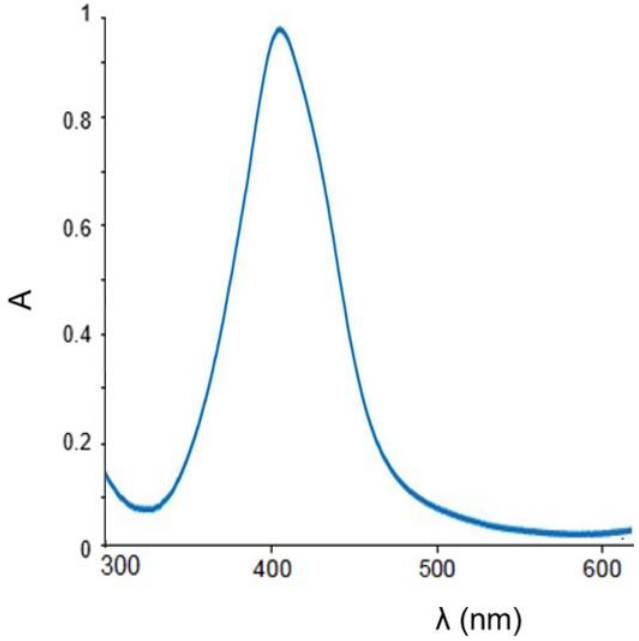


Figure 2.7.2.1. UV-Vis absorption spectrum of the PVP/AgNPs in EG with maximum absorption at 401 nm.

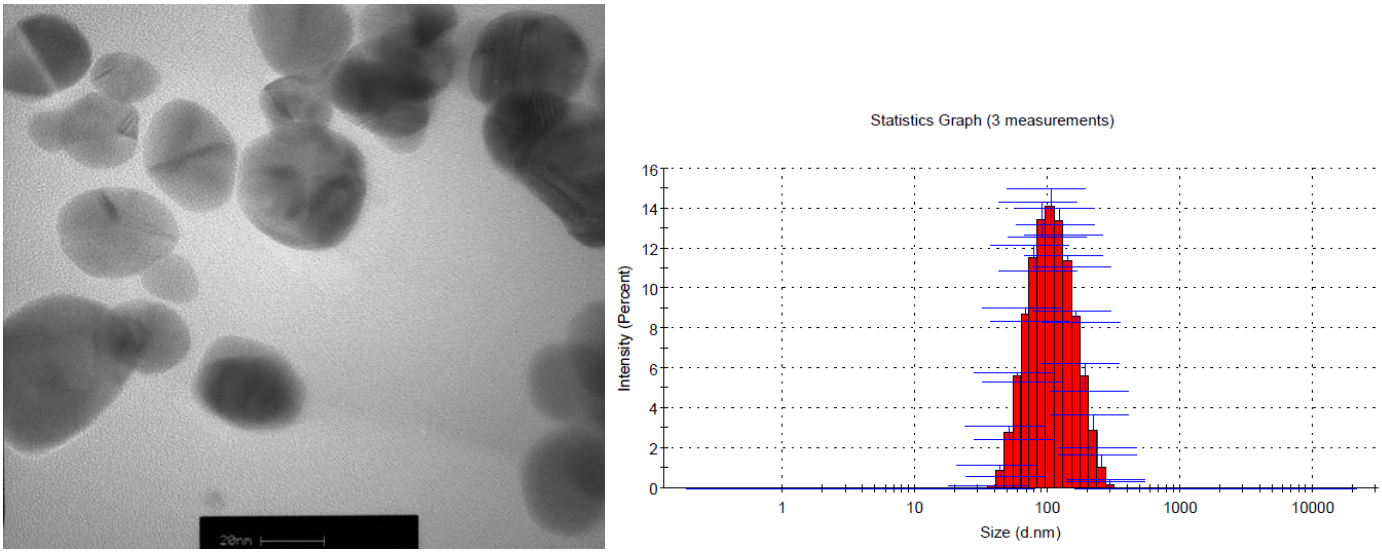
Batches matching the PVP/AgNP literature spectrum were combined into a 0.7 L dispersion containing 6.04 mmol Ag along with 14.47 g PVP and 700 mL EG. For dosing, the dispersion was diluted to 5 L with DI. The stability of PVP/AgNPs was tested over 5 days in DI, DW and RH and was found to be stable (Table S2.7.2).

Table S2.7.2. PVP/AgNP stability over 5 days.

Absorbance	DI	DW	RH
Starting value	0.445	0.746	0.322
After 5 days	0.33	0.789	0.319
Change (%)	-25.9	5.7	2.9

To evaluate the influence of EG in the ozonation/AOP of PVP/AgNPs, the dispersant EG was replaced by DI. Therefore, 18 mL of the synthesized PVP/AgNPs were mixed with three times the volume of acetone to precipitate the NPs. The mixture was then centrifuged at 1300 min^{-1} for 30 min and the supernatant was discarded. The residue was then redispersed in 136 mL DI.

TEM revealed that the PVP/AgNPs had a diameter of 20 to 40 nm for the silver core (Figure S2.7.2.2a). DLS revealed a broad, monomodal distribution with a z-average of 94 nm (Figure S2.7.2.2b).



(a) **(b)**

Figure S2.7.2.2 **(a)** TEM of PVP-40kDa/AgNPs in EG/water; **(b)** Size distribution PVP/AgNPs with DLS at 25.0 °C in (a) EG/water

To investigate the difference between PVP/AgNPs dispersed in ethylene glycol and water, 18 mL of synthesized PVP/AgNPs were mixed with 54 mL of acetone. The suspension was centrifuged at 1300 rpm for 30 minutes, and the solid was separated by decantation and finally redispersed in 136 mL DI.

S2.8 Synthesis of PVP-coated Prussian Blue nanoparticles (Uemura et al., 2004) [9]

PVP-stabilized Prussian Blue nanoparticles were synthesized by preparing a solution of 0.1 mM potassium hexacyanoferrate(III) in 2 mL DI. This solution was slowly added to a vigorously stirred mixture (8 mL) containing 0.1 mM $FeCl_2$ * 4 H_2O and 2 mM PVP (Mw 40 kDa). The color of the solution immediately turns blue due to the formation of mixed-valence potassium hexacyanoferrate(II)/(III) nanoparticles.

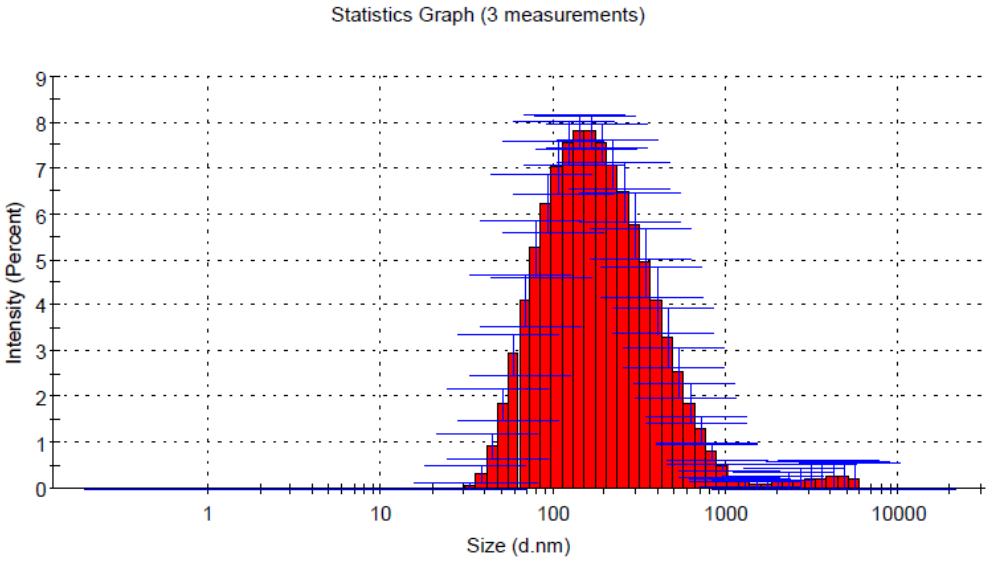


Figure S2.8. Size distribution PVP/PBNPs with DLS in water at 25.0 °C.

Due to low stability, TEM did not show any nanoparticles. DLS revealed a broad, monomodal distribution (Figure S2.8) with a Z-average of 136 nm.

References

[1] McFarland, A. D.; Haynes, C. L.; Mirkin, C. A.; Van Duyne, R. P.; Godwin, H. A. Color my nanoworld. *Journal of Chemical Education* **2004**, *81* (4), 544A. https://doi.org/10.1021/ed081p544a.

[2] Yonezawa, T.; Kunitake, T. Practical preparation of anionic mercapto ligand-stabilized gold nanoparticles and their immobilization. *Colloids and Surfaces. A, Physicochemical and Engineering Aspects* **1999**, *149* (1–3), 193–199. https://doi.org/10.1016/s0927-7757(98)00309-4.

[3] Brubaker, J. Synthesis and Characterization of Gold Nanosalts. Bachelor Thesis, Wittenberg University, Springfield, Ohio, 2006, available online: https://etd.ohiolink.edu/acprod/odb_etd/ws/send_file/send?accession=wuhonors1148584040&disposition=inline, accessed on 17-05-2024.

[4] Pan, Y.; Neuss, S.; Leifert, A.; Fischler, M.; Wen, F.; Simon, U.; Schmid, G.; Brandau, W.; Jahnen-Dechent, W. Size-Dependent cytotoxicity of gold nanoparticles. *Small* **2007**, *3* (11), 1941–1949. https://doi.org/10.1002/smll.200700378.

[5] Tiwari, N. R.; Rathore, A.; Prabhune, A.; Kulkarni, S. K. Gold Nanoparticles for Colorimetric detection of hydrolysis of antibiotics by penicillin G acylase. *Advances in Bioscience and Biotechnology* **2010**, *01* (04), 322–329. https://doi.org/10.4236/abb.2010.14042.

[6] Joshi, N. Gold Nanoparticles and Their Polymer Composites: Synthesis Characterization and Applications, Master Thesis, University of Florida, Florida, 2010, available online: https://digitalcommons.usf.edu/etd/3516, accessed on 17-05-2024.

[7] Elechiguerra, J. L.; Burt, J. L.; Morones, J. R.; Camacho-Bragado, A.; Gao, X.; Lara, H. H.; Yacaman, M. J. Interaction of silver nanoparticles with HIV-1. *Journal of Nanobiotechnology* **2005**, *3*, 6. https://doi.org/10.1186/1477-3155-3-6.

[8] Carotenuto, G.; Pepe, G. P.; Nicolais, L. Preparation and characterization of nano-sized Ag/PVP composites for optical applications. *The European Physical Journal. B, Condensed Matter Physics/European Physical Journal. B, Condensed Matter and Complex Systems* **2000**, *16* (1), 11–17. https://doi.org/10.1007/s100510070243.

[9] Uemura, T.; Ohba, M.; Kitagawa, S. Size and surface effects of Prussian blue nanoparticles protected by organic polymers. *Inorganic Chemistry* **2004**, *43* (23), 7339–7345. https://doi.org/10.1021/ic0488435.

S3. Chemical analyses of river Rhein, raw water, and drinking water [1]

Parameter [2]	River Rhein (RH)	Raw water (RW)	Drinking water (DW)
Temperature (°C)	13.8	13.9	13.5
pH	8.0	7.4	7.6
Oxygen (mg/L)	12.2	3.8	6.5
Electric conductivity (µS/cm)	547	743	825
Turbidity (NTU)	14	0.10	0.01
Alkalinity to pH 4.3 (mmol/L)	2.8	3.2	3.5
Calcium (mg/L)	67	83	87
Magnesium (mg/L)	11	12	12
Sodium (mg/L)	27	46	42
Potassium (mg/L)	3.7	4.4	4.4
Ammonia (mg/L)	0.06	<0.02	<0.02
Nitrite (mg/L)	0.05	<0.02	<0.02
Iron (mg/L)	0.27	0.05	<0.02
Manganese (mg/L)	0.053	0.15	<0.005
Nitrate (mg/L)	9.8	16.0	15.0
Sulphate (mg/L)	47	66	65
Chloride (mg/L)	52.5	92	82
Fluoride (mg/L)	0.11	0.16	0.18
Phosphate total (mg/L)	0.24	<0.1	<0.1
Total organic carbon (mg/L)	2.9	1.0	<0.3
Ionic strength (mM), calculated	8.1	11	10

[1] Average values during the trial phases. [2] Methods employed were according to the German standard methods for the examination of water, wastewater and sludge.

S4. Detailed description of the sampling points in the pilot-scale plant

Sampling point	Description	Remark
CAE	Aeration, storage tank	
MPP	Outlet multiphase pump	
CO0	Inlet continuous flow reactor (CFR)	bottom
CO1	CFR, 1. sampling point	89 cm from bottom
CO2	CFR, 2. sampling point	139 cm from bottom
CO3	CFR, 3. sampling point	189 cm from bottom
CO4	CFR, 4. sampling point	239 cm from bottom
CO5	CFR, 5. sampling point	319 cm from bottom
CF1/1	Anthracite filter layer, 1. sampling point	35 cm from upper filter layer
CF1/2	Anthracite filter layer, 2. sampling point	65 cm from upper filter layer
CF1/3	Sand filter layer, 3. sampling point	95 cm from upper filter layer
CF1/4	Sand filter layer, 4. sampling point	125 cm from upper filter layer
CAF2	Drain anthracite sand filter, line 2	155 cm from upper filter layer, 20 cm gravel, and Klöpper bottom (20 cm height)

S5. Basic parameters of the ozonation reactor and the two-layer filter

To determine the residence times in the continuous flow ozonation reactor (Figure 3, 2.3), 1.0 L of saturated sodium chloride solution (350 g/L) was sucked into the water flow at the H_2O_2 dosing point for 75 s and the conductivities were measured at the CO1 to CO5 sampling points according to Table S4. The experiments were conducted with and without oxygen supply, corresponding to active ozonation.

Table S5.1. Residence times in ozonation continuous flow reactor.

Flow (m^3)	Sampling point	Volume up to sampling point (L)	Most likely residence time [1] (min)	Most likely residence time [1] (min)	Difference (%)
			with oxygen (20 L/h)	without oxygen	
2.00	CO1	240	6.5	4.7	8.2
2.00	CO2	386	8.0	7.0	3.3
2.00	CO3	532	11.5	10.0	3.5
2.00	CO4	678	14.8	14.0	1.4
2.00	CO5	911	20.3	21.7	-1.6

[1] Most likely residence time: peak maximum with salt dosage

The particle retention of a flushed anthracite sand filter was measured with a particle counter in the range of 0.9 to 10 µm and the filter efficiency was calculated. A reduction of 0.7–0.8 LOG levels corresponds to the empirical values for a two-layer filter.

Table S5.2. Filter efficiency of anthracite sand filter.

Particle size (µm)	0.9	1	2	3	4	5	6	7	8	9	10
Inlet average particle number	180.1	152.8	59.3	40.6	30.4	23.6	16.6	12.2	9.0	6.9	5.1
Outlet average particle number	30.8	24.5	7.3	5.6	4.8	4.3	3.9	3.5	3.2	3.0	2.7
Filter efficiency (%)	83	84	88	86	84	82	77	71	64	56	47
Reduction LOG levels	0.77	0.79	0.91	0.86	0.81	0.74	0.63	0.54	0.45	0.35	0.27

To determine the residence times in the anthracite sand filter, 0.2 L of saturated sodium chloride solution (350 g/l) was sucked into the water stream at the pump via a bypass and the conductivities were measured at CF2/1 to CAF2 at the sampling points listed in Table S4 and the maximum values were evaluated.

Table S5.3. Residence time on the anthracite sand filter.

Sampling point	Most likely residence time (min)
CF2/1	6
CF2/2	8
CF2/3	10
CF2/4	12
CAF2	20

S6. Adsorptives and adsorbents for laboratory breakthrough testing of ENPs

Table S6.1. Adsorbates used for breakthrough curves.

Adsorptive	Concentration
Chromium(III) chloride (Tracer)	0.01 mol/L, 2.66 g/L
PVP-55kDa/AuNPs	Diluted 1:4, 0.0746 mmol/L, 14.7 mg/L Au
PVP-55kDa/AuNPs	Diluted 1:100, 0.0167 mmol/L, 3.29 mg/L Au
CTAB/AuNPs	Diluted 1:4, 0.0381 mmol/L, 7.50 mg/L Au
PVP-40kDa/AgNPs in EG [1]	Diluted 1:100, 0.0728 mmol/L, 7.85 mg/L Ag
PVP-40kDa/AgNPs in DI [1]	Diluted 1:100, 0.0728 mmol/L, 7.85 mg/L Ag

[1] To determine retention on anthracite

Table S6.2. Adsorbents used for breakthrough curves.

Packing	Adsorbent data	Flow (mL/min)	Mobile phase
Quartz sand, washed, sterile	10 g Aquagran ® sand, 0.7 – 1.25 mm, 1.08 mm (95 %)	0.8	DW
Rhine sand	10 g River bank sand, 0 – 2 mm, fresh	0.8	RH
Silica gel	0.50 g, pore size 0.6 nm, 40 – 60 µm particle size	2.0	RH
Anthracite (new)	3.15 g, Aquazit ®, type N, 1.4 – 2.5 mm	2.0	RH
Anthracite (used)	3.40 g, Aquazit ®, type N, 1.4 – 2.5 mm used for 2 years in the pilot plant	2.0	RH
Activated wood based charcoal	0.5 g Norit ROW 0.8 SUPRA, 1 µm (46.4 %)	2.0	DW

Table S6.3. Column characteristics for anthracite and sand fillings.

Material	Quartz sand	Anthracite (fresh)
Chemical composition	>96% SiO_2	92% C
Bulk density (kg/m³)	1430	700
Specific density (g/cm³)	2.65	1.35 – 1.55
Effective grain diameter d_{10} (mm)	0.76	1.5 – 1.6
Oversize/ undersize grain (%)	<5	<5
Porosity [1]	0.43	0.56
Bed height (m)	0.033	0.023
column diameter (m)	0.015	0.015
Bed volume (m³)	$5.83*10^{-6}$	$4.06*10^{-6}$

[1] Porosity was determined gravimetrically for the filter by adding water to the packed column until it was saturated without bubbles. Porosity was calculated by dividing the volume of water in the pores by the volume of filter material.

S7. Nanoparticle dilutions used for flocculation

Nanoparticles	Dilution/concentration [1]
PVP/AuNPs	Diluted 1:250, 1.3 mg/L Au
PVP/AgNPs in EG	Diluted 1:250, 0.78 mg/L Ag
PVP/AgNPs in DI	Diluted 1:250, 0.41 mg/L Ag

[1] The dilution medium was DW

S8. Stability of the citrate-coated AuNPs

Table S8. Stability of CA/AuNPs in DI.

CA/AuNPs	λ_{max} (nm)	Absorbance
1st day	519	0.30
3rd day	519	0.31
9th day	519	0.30

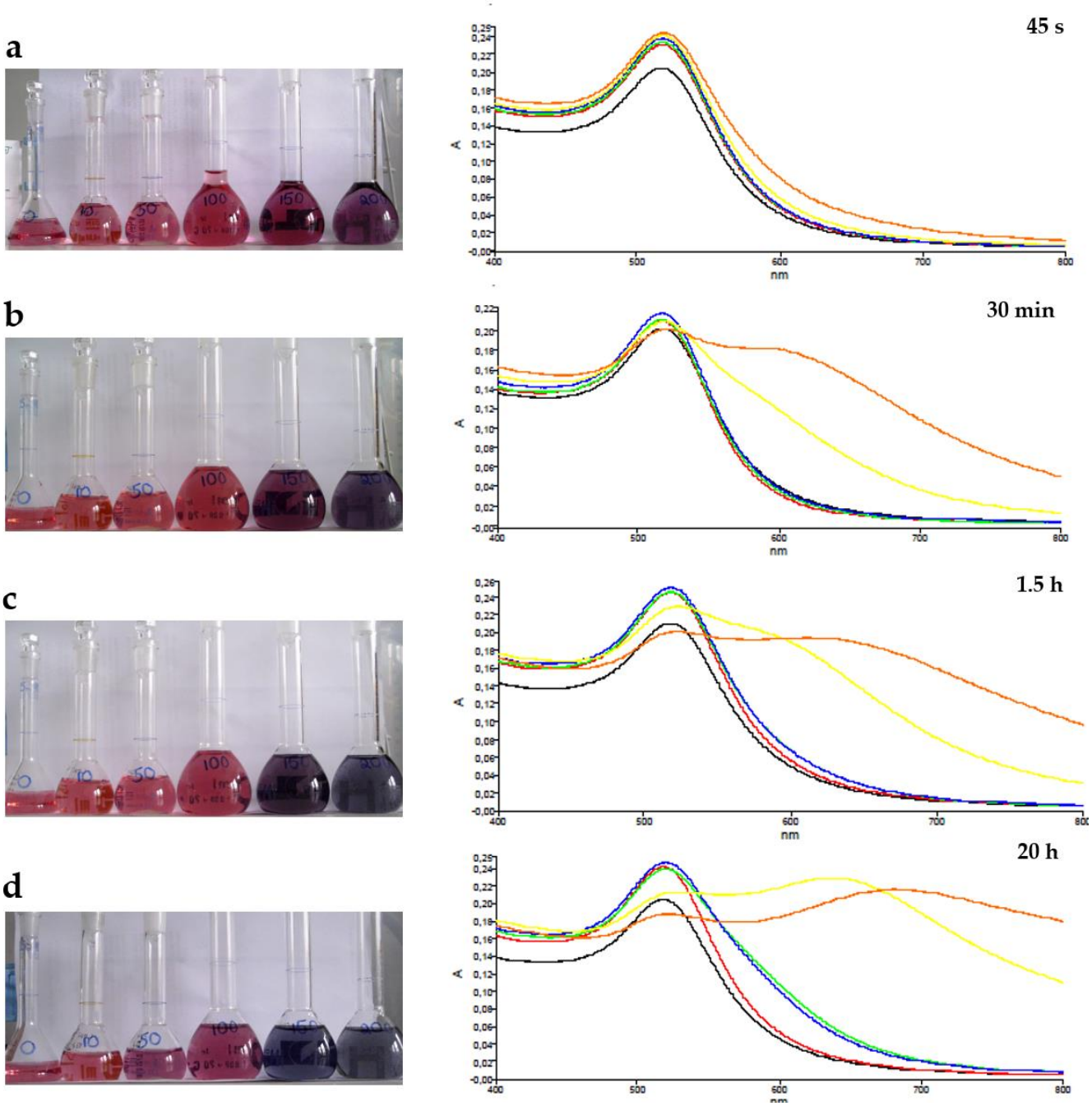


Figure S8. Influence of Ca^{2+} concentration on the CA/AuNP UV-Vis spectrum. **(a)** Shortly after addition (45 s), **(b)** After 30 min, **(c)** after 1.5 h and **(d)** after 20 h; Solutions represented the Ca^{2+} concentrations: 0 mg/ L (black), 0.6 mg/ L (red), 1.4 mg/ L (green), 2.7 mg/ L (blue), 4.1 mg/ L (yellow) and 5.5 mg/ L (orange) from left to right.

S9. Stability of the MPA-coated AuNPs

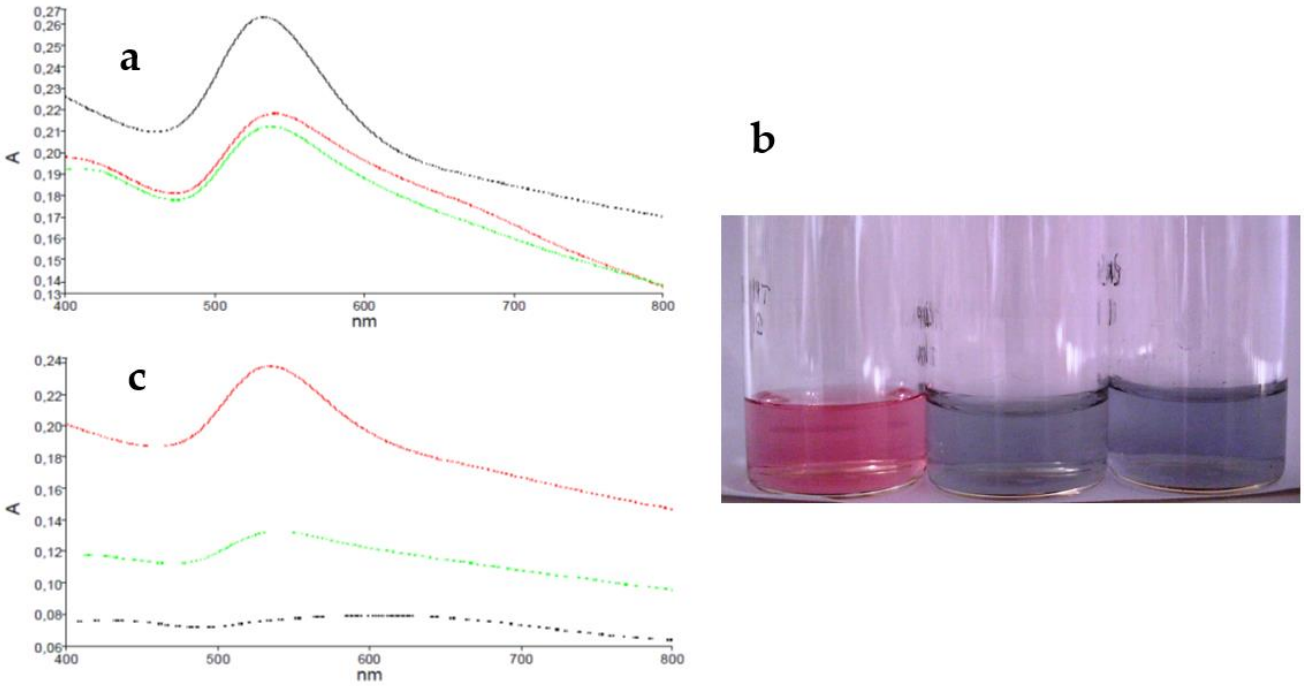


Figure S9. Effect of DW and RH on MPA/AuNPs. **(a)** UV-Vis spectra of the diluted MPA/AuNPs dispersion in DI (black), DW (red) and RH (green); **(b)** MPA/AuNPs diluted in DI, DW and RH (from left to right); **(c)** UV-Vis absorption spectra of MPA/AuNPs in DI (red), DW (black) and RH (green) on the following day.

Table S9. UV-Vis spectral data of MPA/AuNPs diluted in DI, DW and RH.

Time (h)	λ_{max} (nm)	Absorbance	λ_{max} (nm)	Absorbance	λ_{max} (nm)	Absorbance
	DI		DW		RH	
1	533	0.39	540	0.22	537	0.21
24	534	0.24	600	0.21	540	0.13

S10. Stability of MES-coated AuNPs

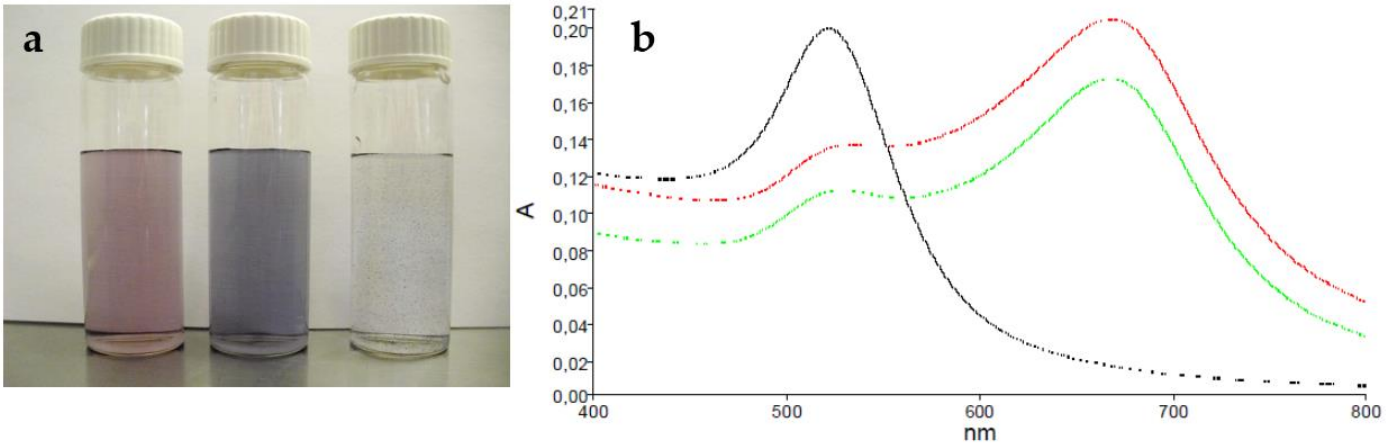


Figure S10. Effect of DW and RH on MES-coated AuNPs. **(a)** MES/AuNPs dispersion diluted in DI, DW and precipitated in DW (from left to right); **(b)** UV-VIS absorption spectra of the diluted MES/AuNPs in DI (black), DW (red) and RH (green).

Table S10. UV-Vis spectral data of MES/AuNPs diluted in DI, DW and RH.

MES/AuNPs	λ_{max} (nm)	Absorbance
DI	522	0.20
DW	538 / 669	0.14/ 0.21
RH	531/ 667	0.11/ 0.17

S11. Stability of TPPMS-coated AuNPs

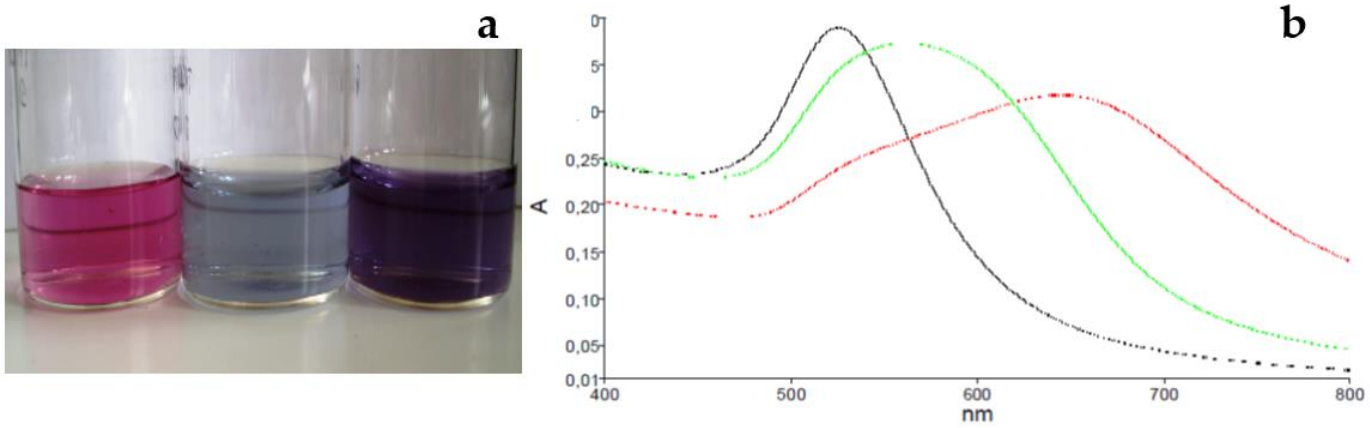


Figure S11. Effect of DW and RH on TPPMS-coated AuNPs. **(a)** TPPMS/AuNPs dispersion diluted in DI, DW and RH (from left to right); **(b)** UV-Vis absorption spectra of the diluted TPPMS/AuNPs in DI (black), DW (red) and RH (green).

Table S11. UV-Vis spectral data of TPPMS/AuNPs diluted in DI, DW and RH.

TPPMS/AuNPs	λ_{max} (nm)	Absorbance
DI	525	0.39
DW	646	0.32
RH	560	0.37

S12. Stability of PVP-coated Prussian Blue NPs

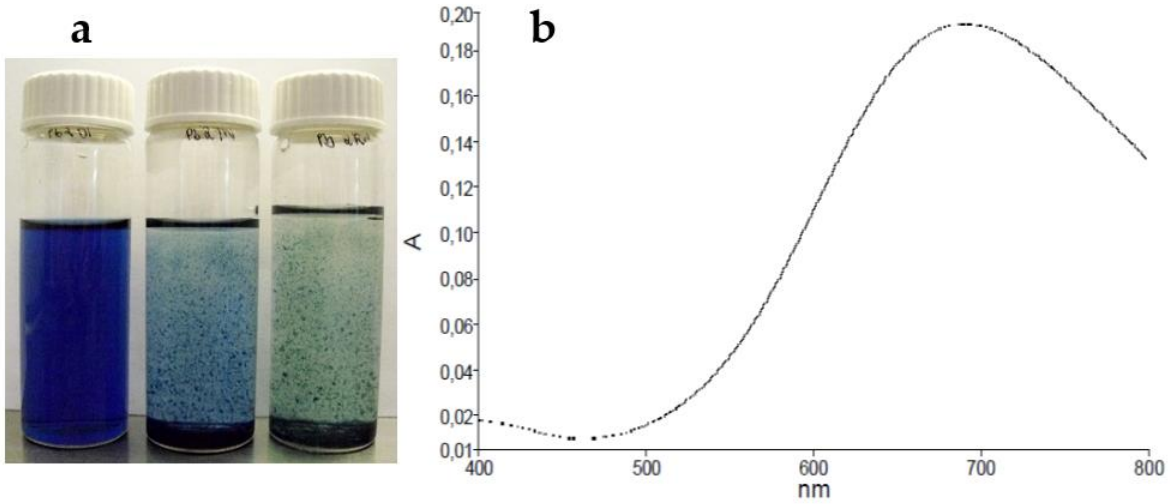


Figure S12. PVP/PBNPs in different types of water. **(a)** Synthesized PVP/PBNPs diluted with DI, DW and RH (from left to right) ; **(b)** UV-Vis absorption spectrum of the diluted PVP/PBNPs in DI.

S13. Data for the evaluation of adsorption isotherms of PVP/AgNPs on sand

Sand (g)	λ_{max} (nm)	Absorbance	c_{eq} (mg/ L)	$1/c_{eq}$ (L/mg)	q_{eq} [1] (mg/g)	$1/q_{eq}$ (g/mg)	ln c_{eq}	ln q_{eq}
0	414.44	0.40	5.050					
5.06	414.36	0.02	0.253	3.96	1.90 E-02	52.7	-1.38	-3.96
2.99	414.87	0.06	0.758	1.32	2.87 E-02	34.8	-0.28	-3.55
1.03	415.65	0.08	1.01	0.99	7.84 E-02	12.8	0.01	-2.55
0.127	416.95	0.17	2.15	0.47	4.57 E-01	2.19	0.76	-0.78
0.016	415.89	0.24	3.03	0.33	2.53 E+00	0.40	1.11	0.93

[1] Calculated silver equilibrium concentration on sand.

S14. Adsorption isotherm of PVP/AgNPs on sand

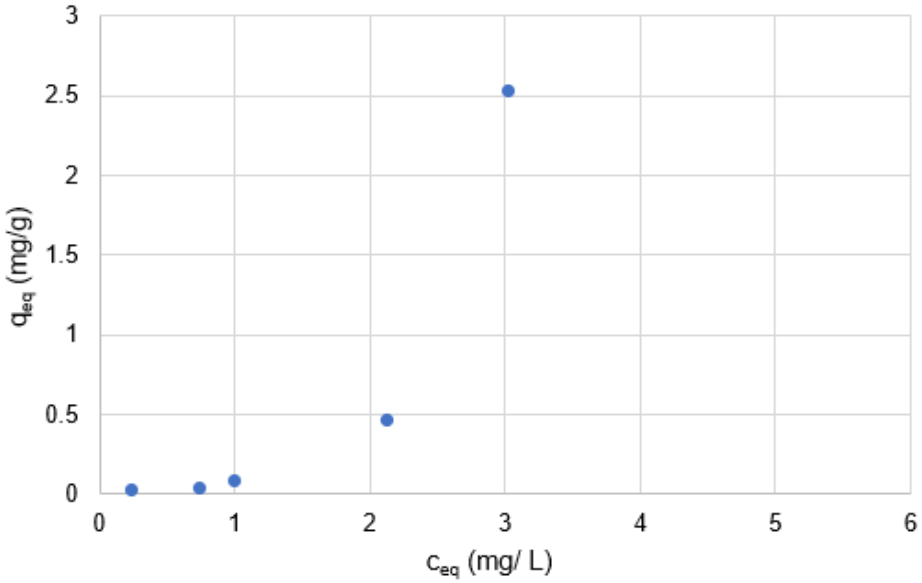


Figure S14. Adsorption isotherm of PVP/AgNPs as Ag on sand.

S15. Data for the evaluation of adsorption isotherms of PVP/AgNPs on silica gel

Silica gel (g)	λ_{max} (nm)	Absorb-ance	c_{eq} (mg/ L)	$1/c_{eq}$ (L/mg)	q_{eq} [1] (mg/g)	$1/q_{eq}$ (g/mg)	ln c_{eq}	ln q_{eq}
0	412.43	0.4	5.0500					
0.001	414.79	0.01	0.1263	7.92	98	0.010	-2.069	4.590
0.0008	412.24	0.03	0.3788	2.64	117	0.009	-0.971	4.760
0.0005	414.98	0.04	0.5050	1.98	182	0.006	-0.683	5.203
0.0003	411.74	0.05	0.6313	1.58	295	0.003	-0.460	5.686
0.0002	408.95	0.08	1.0100	0.99	404	0.002	0.010	6.001

[1] Calculated silver equilibrium concentration on silica gel.

S16. Adsorption isotherm of PVP/AgNPs on silica gel

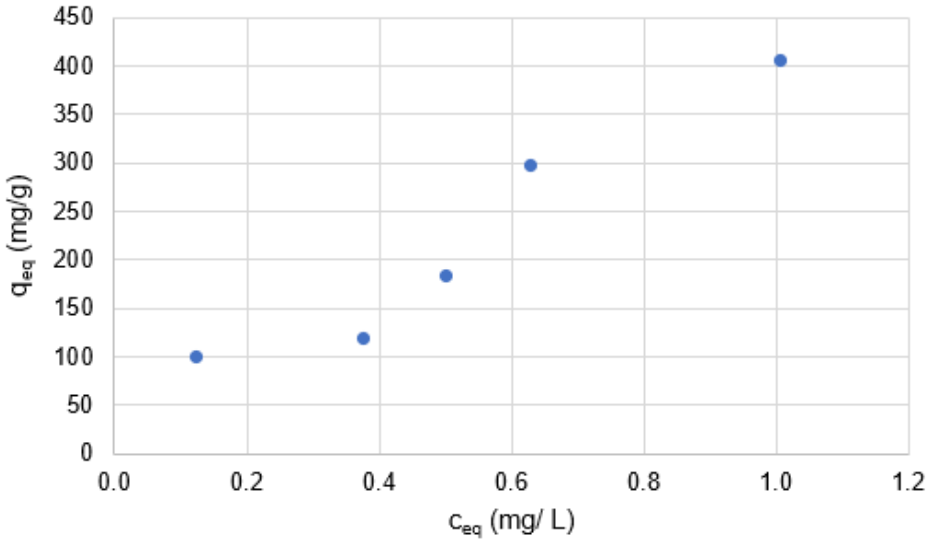


Figure S16. Adsorption isotherm of PVP/AgNPs as Ag on silica gel.

S17. Results of breakthrough behavior of stable nanoparticles

Table S17.1. Parameters of the breakthrough curves for a 10 g quartz sand bed.

Adsorptive	t_B (h)	t_S (h)	$t_{0.5}$ (h)	$\eta_{i,Ads}$ (%)
Tracer ($CrCl_3$)	0.12	0.31	0.15	75
CTAB/AuNPs	0.10	0.75	0.16	50
PVP/AuNPs	0.09	0.36	0.15	63
PVP/AgNPs	0.10	0.97	0.13	47

Table S17.2. Parameters of the breakthrough curves for a 10 g Rhine sand bed.

Adsorbate	t_B (h)	t_S (h)	$t_{0.5}$ (h)	$\eta_{i,Ads}$ (%)
Tracer ($CrCl_3$)	0.13	0.30	0.17	72
CTAB/AuNPs	0.42	5.6	1.4	24
PVP/AuNPs	0.10	0.30	0.13	68
PVP/AgNPs	0.11	0.60	0.21	43

Table S17.3. Parameters of the breakthrough curves for a 0.5 g silica gel bed.

Adsorbate	t_B (h)	t_S (h)	$t_{0.5}$ (h)	$\eta_{i,Ads}$ (%)
Tracer ($CrCl_3$)	0.01	0.05	0.02	54
PVP/AuNPs	0.12	0.24	0.17	69
PVP/AgNPs in EG	0.06	0.16	0.09	68
PVP/AgNPs in DI	0.10	0.18	0.15	66

Table S17.4. Parameters of the breakthrough curves for a 0.5 g active carbon bed (ROW 0.8 Supra).

Adsorbate	t_B (h)	t_S (h)	$t_{0.5}$ (h)	$\eta_{i,Ads}$ (%)
Tracer ($CrCl_3$)	0.05	0.08	0.06	83
CTAB/AuNPs	0.97	1.29	1.12	86
PVP/AuNPs	0.05	0.14	0.07	62
PVP/AgNPs	0.85	4.66	2.18	35

Table S17.5. Parameters of the breakthrough curves for a fresh anthracite bed (3.15 g).

Adsorbate	t_B (h)	t_S (h)	$t_{0.5}$ (h)	$\eta_{i,Ads}$ (%)
Tracer ($CrCl_3$)	0.04	0.07	0.05	78
PVP/AuNPs	0.08	0.43	0.21	38
PVP/AgNPs in EG	0.08	0.64	0.34	22
PVP/AgNPs in DI	0.03	0.73	0.41	8

Table S17.6. Parameters of the breakthrough curves for an used anthracite bed (3.40 g).

Adsorbate	t_B (h)	t_S (h)	$t_{0.5}$ (h)	$\eta_{i,Ads}$ (%)
Tracer ($CrCl_3$)	0.03	0.06	0.04	66
PVP/AuNPs	0.14	0.86	0.42	33
PVP/AgNPs in EG	0.08	0.94	0.38	20
PVP/AgNPs in DI	0.25	1.92	1.08	23

S18. Flocculation results of ENPs with Trifloc® and Gilufloc®

Nanoparticles	Flocculant	c(flocculant) (mg/L)	Removal of NPs [1,2] after 17 min (%)	Removal of NPs [1,2] after 32 min (%)
PVP/AuNPs in water (1.3 mg/L Au)	Trifloc® as Fe(III)	1	32	21
		5	20	43
		10	47	36
		50	95	90
	Gilufloc® as Al_2O_3	1	16	7
		5	<1	27
		10	34	23
		50	61	51
PVP/AgNPs in water with EG (0.78 mg/L Ag)	Trifloc® as Fe(III)	1	57	91
		5	96	97
		10	97	99
		50	79	69
	Gilufloc® as Al_2O_3	1	70	56
		5	85	93
		10	78	94
		50	88	91
PVP/AgNPs in water (0.41 mg/L Ag)	Trifloc® as Fe(III)	1	87	68
		5	59	63
		10	87	76
		50	18	77
	Gilufloc® as Al_2O_3	1	95	23
		5	96	83
		10	76	64
		50	96	73

[1] based on the metal content. Green colored background: reduction ≥90%. [2] The relative combined uncertainty of the removal is estimated to be ~ 7% with the standard deviation of two photometric measurements multiplied by the statistical factor of 3.

S19. Test conditions during ozonation and AOP of PVP/AuNPs

Parameter	Adjusted value
Raw water flow	2.0 m^3/h
Ozone dose	585 ppb
PVP/AuNP pump rate	7.2 L/h
AuNP concentration	3.09 mmol/L Au
Residual ozone before dosing (CO5)	500 ppb
Residual ozone during dosing (CO5)	460 ppb
Parameter AOP	
Raw water flow	2.0 m^3/h
Ozone dose	585 ppb
PVP/AuNP pump rate	7.2 L/h
Flow rate H_2O_2 (1%)	0.42 L/h
AuNP concentration	3.09 mmol/L Au
Residual ozone before dosing	12 ppb

S20. Retention data of PVP/AuNP on the two-layer filter

CO5		CF2/1		CF2/2	
Time (min)	**Absorbance**	**Time (min)**	**Absorbance**	**Time (min)**	**Absorbance**
15	0.0044	30	0.00355	40	0.00188
20	0.0033	35	0.00204	45	0.00247
25	0.0037	40	0.00263	50	0.00119
30	0.0022	45	0.00247	55	0.00335
35	0.0026	50	0.00119		
Mean	0.0032		0.0024		0.0022
Standard deviation	0.0009		0.0009		0.0009

CF2/3		CF2/4		CAF2	
Time (min)	**Absorbance**	**Time (min)**	**Absorbance**	**Time (min)**	**Absorbance**
50	0.0022	60	0.0017	65	0.0086
55	0.0030	65	0.0034	70	0.0064
60	0.0021	70	0.0065	75	0.0056
65	0.0014	75	0.0061	80	0.0049
				85	0.0040
				90	0.0025
Mean	0.0022		0.0044		0.0053
Standard deviation	0.0006		0.0023		0.0021

S21. Evaluation of PVP/AuNP retention on the two-layer filter

Sampling point	A_{mean}	Sd of A_{mean}	Retention A_{mean} [1]	Retention A_{mean}(%) [1]
CO5	0.0032	0.0009		
CF2/1	0.0024	0.0009	0.00005	25.8
CF2/2	0.0022	0.0009	-0.00082	30.5
CF2/3	0.0022	0.0006	-0.00098	32.3
CF2/4	0.0044	0.0023	-0.00104	-37.8
CAF2	0.0053	0.0021	0.00121	-66.8

[1] based on CO5.

Sampling point	A_{max}	Retention A_{max} [1]	Retention A_{max} (%) [1]
CO5	0.0044		
CF2/1	0.0036	-0.0396	19.3
CF2/2	0.0034	-0.0405	23.9
CF2/3	0.0030	-0.0407	32.7
CF2/4	0.0065	-0.0410	-48.6
CAF2	0.0086	-0.0375	-96.4

[1] based on CO5 with equation 2.

S22. Test conditions during ozonation and AOP of PVP/AgNPs

Parameter	Adjusted value
Raw water flow	2.0 m^3/h
Ozone dose	445 ppb
PVP/AgNP pump rate	15 L/h
AgNP concentration	0.85 mmol/L Ag
Residual ozone before dosing (CO5)	116 ppb
Residual ozone during dosing (CO5)	0 ppb
Parameter AOP	
Raw water flow	2.0 m^3/h
Ozone dose	445 ppb
PVP/AgNP pump rate	15 L/h
Flow rate H_2O_2 (1%)	0.42 L/h
AgNP concentration	0.85 mmol/L Ag
Residual ozone before dosing (CO0)	12 ppb

S23. Influence of PVP/EG on residual ozone

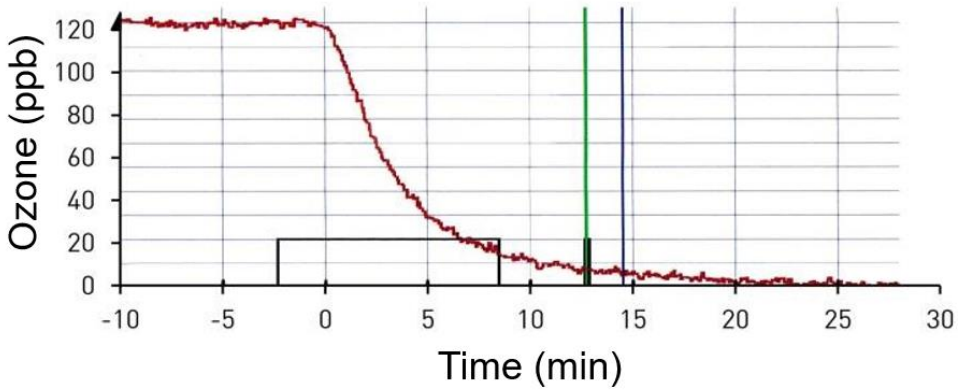


Figure S23. Evolution of residual ozone concentration at CO5 (red curve) during dosing of PVP dissolved in ethylene glycol (black box).

S24. Retention data of PVP/AgNPs on the two-layer filter

CO5		**CF2/1**		**CF2/2**	
Time (min)	**Absorbance**	Time (min)	**Absorbance**	**Time (min)**	**Absorbance**
20	0.04661	30	0.02392	40	0.02211
25	0.05580	35	0.02367	45	0.01627
30	0.04795	40	0.02598	50	0.01957
35	0.04494	45	0.02325	55	0.01732
Mean	0.0488		0.0242		0.0188
Standard deviation	0.0048		0.0012		0.0026

CF2/3		**CF2/4**		**CAF2**	
Time (min)	**Absorbance**	**Time (min)**	**Absorbance**	**Time (min)**	**Absorbance**
50	0.00543	60	0.00284	65	0.00396
55	0.00377	65	0.00343	70	0.00496
60	0.00524	70	0.00252	75	0.00352
65	0.00414	75	0.00218	80	0.00179
				85	0.00131
Mean	0.0046		0.0027		0.0031
Standard deviation	0.0008		0.0005		0.0015

S25. Evaluation of PVP/AgNP LSPR retention on the two-layer filter

Sampling point	A_{mean}	Sd of A_{mean}	Retention A_{mean}	Retention A_{mean}(%) [1]
CO5	0.0488	0.0048		
CF2/1	0.0242	0.0012	0.00002	50.4
CF2/2	0.0188	0.0026	-0.02460	61.5
CF2/3	0.0046	0.0008	-0.02998	90.5
CF2/4	0.0027	0.0005	-0.04416	94.4
CAF2	0.0031	0.0015	-0.04606	93.6

[1] Based on CO5 with equation 2.

Sampling point	A_{max}	Retention A_{max}	Retention A_{max} (%) [1]
CO5	0.0558		
CF2/1	0.0260	0.0298	53.4
CF2/2	0.0221	0.0039	60.4
CF2/3	0.0054	0.0167	90.3
CF2/4	0.0034	0.0020	93.9
CAF2	0.0050	-0.0015	91.1

[1] Based on CO5 with equation 2.